STRUCTURAL AND COMPOSITIONAL SPECIFICATIONS ON BIOGENIC FERRIHYDRITE NANOPARTICLES PRODUCTION BY *KLEBSIELLA OXYTOCA*

S. KICHANOV[1], A. PANTELICA[2], D. PANTELICA[2], S. STOLYAR[3,4], R. ISKHAKOV[4], D. ARANGHEL[2,5], P. IONESCU[2], R. VLADOIU[6], M. BALASOIU[1,2,7*]

[1] Joint Institute for Nuclear Research, Dubna, 141980 Moscow Region, Russia
[2] Horia Hulubei National Institute for Physics and Nuclear Engineering, Bucharest-Magurele, Romania
[3] Siberian Federal University, 660041, Krasnoyarsk, Russia
[4] Federal Research Center KSC SB RAS, Krasnoyarsk, Russia
[5] Extreme Light Intrastructure Nuclear Physics (ELI-NP), POB-MG6, Bucharest-Magurele, Romania
[6] Ovidius University, Faculty of Applied Sciences and Engineering, Constanța, Romania
[7] Moscow Technical Physics Institute, Dolgoprudnyi, Russia

*Corresponding author e-mail: balas@jinr.ru

Received

Abstract. Investigations of biogenic ferrihydrite nanoparticles produced by bacteria *Klebsiella oxytoca* by applying methods of synchrotron radiation powder diffraction, particle-induced X-ray emission (PIXE), proton induced gamma-emission (PIGE) and proton Rutherford backscattering (RBS) are reported and discussed.

Key words: Biogenic ferrihydrite, nanoparticles structure, synchrotron radiation powder diffraction, PIXE, PIGE, RBS

1. INTRODUCTION

Development of nanoparticles synthesis techniques with well-defined size, shape and composition is a task and an important area of research. Modern methods of chemical synthesis of nanoparticles are energy intensive, use toxic chemicals and often give particles in nonpolar organic solvents, thereby eliminating the biomedical application. A promising new dimension in this field is the use of microorganisms for the production of inorganic nanoparticles [1, 2].

It is known that many microorganisms produce inorganic nanostructures and nanoparticles with properties similar to chemically synthesized materials, with control over the size, shape and composition of the particles [3].

Ferrihydrite nanoparticles produced by bacteria *Klebsiella oxytoca* in the course of biomineralization of iron salt solutions from natural medium [3, 4] it was

shown that exhibit unique magnetic properties: they are characterized by both the antiferromagnetic order inherent in a bulk ferrihydrite and the spontaneous magnetic moment due to the decompensation of spins in sublattices of nanoparticles [5]. This feature has been recognized as a possible application of magnetic manipulation on these natural objects [5], opening their way to nanomedicine, and biotechnologies [6].

In order to characterize the samples with improved analytical sensitivity a combined use of a few techniques is often required.

Structural properties of biogenic ferrihydrite nanoparticles produced by bacteria *Klebsiella oxytoca* were previously investigated by means of scanning electron microscopy [7], small angle X-ray scattering [7-9], transmission electron microscopy [8], spectroscopic methods (UV-Vis [10, 11], fluorescence emission [11], FT-IR [10, 11]).

In the present work, progress in the investigation of biogenic ferrihydrite nanoparticles produced by bacteria *Klebsiella oxytoca* by applying methods of synchrotron radiation powder diffraction, Proton-Induced X-ray Emission (PIXE), Proton Induced Gamma-Emission (PIGE), and Rutherford Backscattering Spectrometry (RBS) with protons are reported.

2. EXPERIMENTAL

2.1. FERRIHYDRITE SAMPLE PRODUCTION

In this study, the bacterial biomass isolated from the sapropel obtained from the Lake Borovoe (Krasnoyarsk region) was grown under microaerophilic conditions on a Lovley medium of composition (g/L) $NaHCO_3$, 2.5; $CaCl_2 \cdot H_2O$, 0.1; KCl, 0.1; NH_4Cl, 1.5; and $NaH_2PO_4 \cdot H_2O$, 0.6. The ferric citrate concentration was varied from 0.2 to 5 g/L, the yeast extract concentration was 0.05 g/L, and the benzoic acid concentration was varied from 0.2 to 0.5 g/L.

As a result of variation of the growth conditions for the microorganisms (growth period, light exposition, potassium citrate – ferric citrate rate, etc.), bacterium *Klebsiella oxytoca* creates, as was established in previous works [4-7], two types of ferrihydrite nanoparticles (Fe12 and Fe34) whose differences are accurately identified by means of Mössbauer spectroscopy [5] and static magnetic measurements analysis [6], scanning electron microscopy [7] and small angle X-ray scattering [7-9]. Samples Fe12 and Fe34 have been separated from a bacterial biomass grown during 8 and 21 days, respectively.

2.2. SYNCHROTRON RADIATION POWDER DIFFRACTION

Synchrotron radiation sources have several advantages over conventional X-radiation sources, including a wider spectrum and higher luminosity. This is the

reason why synchrotron radiation has been increasingly used in the world to solve a wide spectrum of fundamental and applied problems in physics, chemistry, materials science, biology, medicine and earth sciences. High intensity of the synchrotron radiation beam allows carrying out experiments with small volumes of the investigated matter.

The samples were positioned in a monochromatic beam with a wavelength of 0.586 Å of Mediana station into operation at the Kurchatov Synchrotron Radiation Source (KSRS), Moscow [12].

The data collection of diffraction patterns was done by means of Image plate type detectors. Transformation and the analysis of the received spectra were made with the software package Fit2d and Foolproof.

2.3. ION BEAM ANALYSIS (PIXE, PIGE, RBS)

PIXE, PIGE, and RBS analytical techniques were concomitantly carried out at the 3 MV Tandetron accelerator of the Horia Hulubei National Institute of Physics and Nuclear Engineering (IFIN-HH) in Bucharest-Magurele, using a 3 MeV proton beam extracted from an HVE model 860A Cs sputter ion source and a dedicated Ion Beam Analysis (IBA) reaction chamber [13].

For IBA application, dry powder samples were prepared as pellets of 1 cm diameter and 1 mm thickness (thick targets).

PIXE and PIGE measurements were performed using a normal to the target beam in vacuum, as well as X-ray and gamma-ray Ortec HPGe (High Purity Germanium) detectors oriented at 45^{o} with respect to the thick composite target and beam direction. The X-ray spectrometric chain was based on IGLET-X-06135-S detector of 140 eV resolution at 5.9 keV, while for the gamma-ray spectrometry a GEM10P4-70 detector of 1.75 keV resolution at 1332 keV of ^{60}Co was used.

The beam intensity was kept in the range 1.4–3 nA to maintain a lower than 10 % dead time, which implies low pile-up corrections. The spectra were collected during 0.5 - 1 h. The X- and gamma- ray yields were normalized with respect to the integrated beam current on the target.

GUPIX (Guelph PIXE) programme [14] was used for a quantitative analysis by PIXE. The element concentrations determined in samples were normalized to 100 % total. The light elements H, O, C, and N were introduced in GUPIX fit as invisible component with stoichiometric ratios determined by RBS.

For PIGE, a relative standardization was used [13, 15]. As comparator standards, high purity chemical compounds (NaCl, MgO, and Fe_2P) were chosen to determine Na, Cl, Mg, Fe, and P. Proton beam stopping powers for the biogenic ferrihydrite samples (matrix assessed by RBS and PIXE) and comparator standards were calculated using SRIM software [16]. To determine $E_{1/2}$ proton beam energy in PIGE analysis (energy for which a halved reaction yield is observed), excitation

functions (beam energy between 2.4 and 3 MeV) were measured for the investigated samples and comparator standards [13].

For RBS, the backscattered H particles were detected with a passivated ion implanted silicon detector. The detector had an energy resolution of 16 keV, was placed under an angle of 165º with respect to the incident beam direction and subtended a solid angle of 1.641 msr. To avoid channeling effects, the sample was tilted 7º relative to the beam direction [15].

3. RESULTS AND DISCUSSION

3.1. SYNCHROTRON RADIATION POWDER DIFFRACTION

The diffraction spectrum of biogenic ferrihydrite nanoparticles sample Fe12 obtained at KSRS in Moscow is given in Fig. 1:

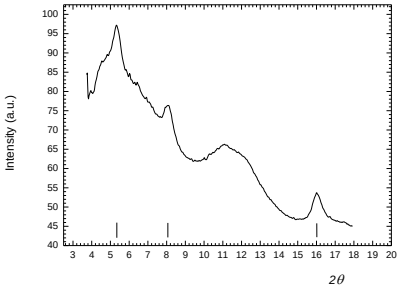

Fig. 1. Diffraction spectrum of biogenic ferrihydrite nanoparticles sample Fe12.

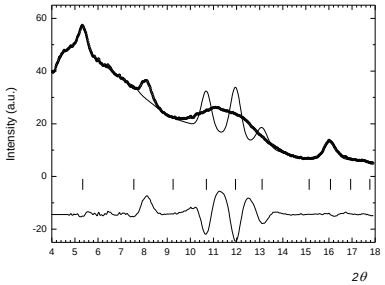

Fig. 2. The processing of diffraction spectrum of sample Fe12 using the model of cubic cell.

Diffraction peaks for this sample are located at scattering angles of $2\theta = 5.4^0$; 8.1^0; 16^0. Besides this, around the scattering angles of $2\theta = 10^0$-13^0 is observed a diffusive halo. The positions of the diffraction peaks which are related to each other as 2:3:6 may correspond to the cubic system. However, in this case, the description yields only the two extreme peaks of the spectrum. These positions are consistent with the values of Miller indices (100) and (300). The peak located at a scattering angle $2\theta = 8.1^0$ is located close to the position corresponding to Miller indices (110). Processing result of the obtained diffraction spectrum (Fig. 1) using a cubic cell model is shown in Fig. 2.

A better treatment of the diffraction spectrum of sample Fe12 seems to be the tetragonal cell model use (a=b=5.81Å, c=6.28Å). In this case, the peaks located

at the scattering angle $2\theta = 5.4^0$; 8.1^0; 16^0 are reflections of the interplanar distances with Miller indices (001) (110) and (003), respectively.

In Fig. 3, a region of the diffraction spectrum of sample Fe34 is given. One of the possible descriptions of the structure of this sample is the model using a monoclinic cell (a = 3.79, b = 11.04, c = 10.54, β =95.26). In the diffraction pattern of this sample, one should note the presence of the reflections observed in the spectrum of sample Fe12 at scattering angles $2\theta = 5.4^0$; 8.1^0; 16^0. The processing of the selected region of the diffraction spectrum is shown in Fig. 4.

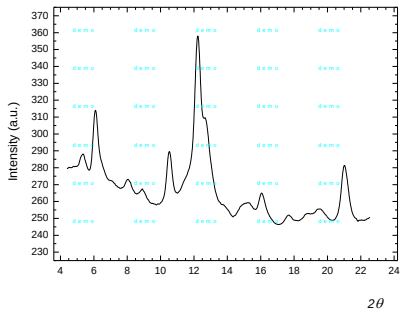

Fig. 3. A section of the experimental diffraction spectrum of sample Fe34.

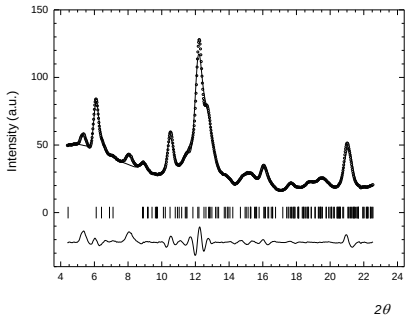

Fig. 4. The processing of diffraction spectrum section of sample Fe34.

3.2. ION BEAM ANALYSIS

PIXE, PIGE, and RBS complementary ion beam techniques were used simultaneously to provide information on elemental content of biogenic ferrihydrite nanoparticles produced by *Klebsiella oxytoca*.

PIXE spectrum (experimental and GUPIX fit values) for Fe12 sample is presented in Fig. 5. PIXE results (expressed in percent dry weight, d.w.) for the Fe12 and Fe34 samples are given in Table 1. Combined counting and fit analytical uncertainties are also given in this table.

A total 14 elements were determined by PIXE in the examined samples, as follows (concentration levels in descending order, in parentheses): Fe, P, Cl, Ca, and K (tens of percent to percent); Hg, Pb, Al, Si, Rb, and S (tenths of percentage); Rb, S, Zn, Cr, and Mn (hundreds of ppm/part per million).

PIGE spectrum for Fe12 sample is shown in Fig. 6. Nuclear reactions of (p,p') type on ^{23}Na, ^{24,25}Mg, ^{31}P, ^{35}Cl, and ^{56}Fe target isotopes and (p,αγ) type on ^{23}Na and ^{31}P isotopes, as well as characteristic gamma lines are also given in Fig. 6. PIGE results obtained for Na, Mg, P, Cl, and Fe (5 elements) in Fe12 and Fe34

samples are presented in Table 2. Analytical uncertainties were calculated based on counting uncertainties for sample and standard, concentration uncertainty for standard, and stopping power ($E_{1/2}$) uncertainty.

Major elements Fe, P, and Cl determined by PIGE (Table 2) were found to be at similar levels with those obtained by PIXE (Table 1). In addition, Na and Mg were measured by PIGE at levels between 0.23 % and 1.8 % d.w.

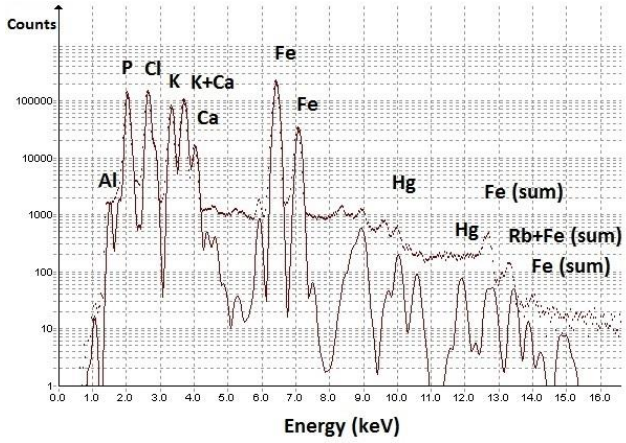

Fig. 5. PIXE spectrum of the Fe12 biogenic ferrihydrite sample and GUPIX fit.

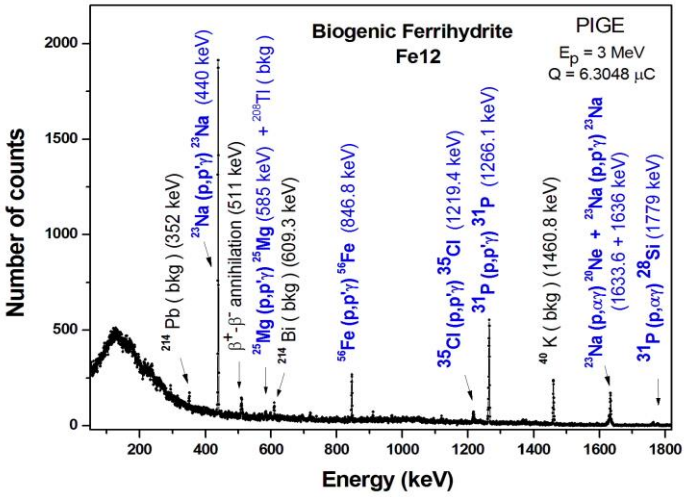

Fig. 6. PIGE spectrum of the Fe12 biogenic ferrihydrite sample.

Table 1. Elemental contents determined by PIXE in the Fe12 and Fe3 biogenic ferrihydrite samples, in percent d.w.

Element	Fe12	Fe34
Al	0.327 ± 0.007	0.356 ± 0.009
Si	0.184 ± 0.008	0.233 ± 0.013
P	12.3 ± 0.1	15.1 ± 0.1
S	< 0.02	0.16 ± 0.02
Cl	11.9 ± 0.1	1.19 ± 0.01
K	6.44 ± 0.02	4.11 ± 0.01
Ca	7.98 ± 0.03	6.67 ± 0.02
Cr	< 0.01	0.027 ± 0.01
Mn	0.094 ± 0.003	< 0.01
Fe	27.0 ± 0.1	32.7 ± 0.1
Zn	0.039 ± 0.010	< 0.03
Rb	0.082 ± 0.016	0.247 ± 0.030
Hg	0.328 ± 0.036	0.684 ± 0.060
Pb	0.197 ± 0.035	0.494 ± 0.064

Table 2. Elemental contents determined by PIGE in the Fe12 and Fe34 biogenic ferrihydrite samples, in percent d.w.

Element	Fe12	Fe34
Na	0.804 ± 0.040	0.234 ± 0.012
Mg	1.82 ± 0.60	1.10 ± 0.64
P	10.5 ± 0.5	11.1 ± 0.6
Cl	7.70 ± 1.00	0.89 ± 0.31
Fe	25.9 ± 1.8	30.9 ± 1.5

RBS spectrum of the Fe12 sample is represented in Fig. 7. Besides light elements (C, N, O) P, Cl, K, Ca, and Fe are also present. The scattering profiles of C, N and O appear at energies of 2.154, 2.258 and 2.337 MeV, respectively, corresponding to the backscattering of the proton beam on the light film components. The scattering profile of Fe starts at 2.792 MeV energy. These energies are in agreement with the energies calculated from kinematics indicating that the elements are present starting from the surface of the sample.

The elemental concentrations summarized in Table 3 were inferred using the simulation code RUMP [17] by fitting the RBS experimental spectrum for the

sample. The hydrogen was introduced in RUMP simulation to obtain a better reproduction of RBS spectrum. Its concentration value reflects the best agreement between the simulated and the measured spectra.

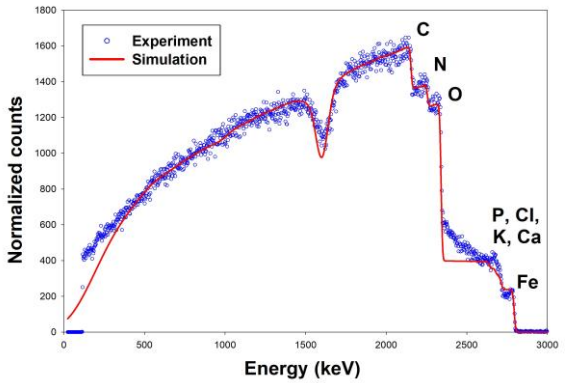

Fig. 7. RBS spectrum of the Fe12 biogenic ferrihydrite sample and RUMP simulation.

Table 3. Elemental contents determined by RBS in Fe12 and Fe34 biogenic ferrihydrite samples (atomic percent and weight percent, d.w.).

Fe12			Fe34		
Elem.	**at.%**	**wt.%**	**Elem.**	**at.%**	**wt.%**
H	45.1	3.61	**H**	40.5	3.08
C	8.5	8.12	**C**	13.2	11.9
N	4.6	5.07	**N**	2.0	2.14
O	28.2	35.9	**O**	30.4	36.7
P	2.6	6.44	**P**	4.8	11.2
Cl	2.4	6.86	**Cl**	0.3	0.92
K	1.3	4.10	**K**	1.0	3.08
Ca	1.7	5.29	**Ca**	1.7	5.06
Fe	5.6	24.6	**Fe**	6.1	25.9

As could be seen in Table 3, the RBS results for P, Cl, K, Ca, and Fe are in agreement with those determined by PIXE and PIGE for Fe12 and Fe34 samples.

Concerning the light elements determined by RBS, similar mass fractions for O in both samples, 1.5 times higher content for C in Fe34, as well as 1.2 and 2.4 times higher contents for H and N in Fe12, respectively, were found.

By comparing the elemental contents determined by PIXE (and PIGE for Na and Mg) in Fe12 and Fe34 biogenic ferrihydrite samples (concentration ratios in parentheses), higher values in Fe34 sample were found for Fe (1.21), P (1.23), Si (1.27), Hg (2.1), Pb (2.5), Rb (3.0), Cr (> 2.7), and S (> 8), while higher values in Fe12 sample were found for Ca (1.2), K (1.6), Mg (1.7), Na (3.4), Cl (10.0), Zn (> 1.3), and Mn (> 9.4).

Metallic element contents, in particular Fe, as well as their mass fractions determined by PIXE, PIGE, and RBS ion beam techniques in Fe12 and Fe34 biogenic ferrihydrite samples, are in agreement with the growing condition of *Klebsiella oxytoca* bacterium, during 8 and 21 days, respectively (higher contents of Fe, P, Si, Hg, Pb, Rb, Cr, and S in Fe34 sample).

4. CONCLUSIONS

Synchrotron radiation powder diffraction measurements of the ferryhydrite Fe12 and Fe34 samples showed different structure, i.e. for Fe12, a tetragonal cell model and for Fe34, a monoclinic cell, respectively, give best fits to the their diffraction spectra.

PIXE non-destructive technique was able to determine 14 elements in total using GUPIX programme. The multi-elemental PIXE analysis showed the investigated biogenic particles to have an unexpectedly high complex composition.

PIGE technique was able to determine 5 elements in total, two of them (Na and Mg) complementary to PIXE. The results obtained for P, Cl, and Fe were in agreement with those measured by PIXE.

RBS was able to put in evidence, besides C, N, O, and H light elements, the presence of P, Cl, K, Ca and Fe, starting from the surface of the sample.

Acknowledgements. This work was supported by the Joint Institute for Nuclear Research Project No. 04-4-1121-2015/2017, and RO-JINR Projects Nos. 95/15.02.2016 and 96/15.02.2016, items 77, 82 and was funded by RFBR and Krasnoyarsk region according to the research project № 17-43-240527. Support by the Special Program for Siberian Federal University of the Ministry of Education and Science of the Russian Federation is acknowledged.

REFERENCES

1. M. Sastry, A. Ahmad, M.I. Khan, R. Kumar, Current Science, 85(2), 162 (2003).
2. S.V. Stolyar, O.A. Bayukov, D.A. Balaev, R.S. Iskhakov, L.A. Ishchenko, V.P. Ladygina, R.N. Yaroslavtsev, Journal of Optoelectronics and Advanced Materials, 17(7-8), 968-972 (2015).
3. M. Balasoiu, A.I. Kuklin, G.M. Arzumanyan, T.N. Murugova, S.V. Stolyar, R.S. Iskhakov, L.A. Ishchenko, Yu.L. Raikher, Biogenic nanoparticles produced by bacteria *Klebsiella oxytoca*: structure investigations. In: Modern Trends in Nanoscience, Ed. Maria Balasoiu and Grigory M. Arzumanyan, The Publishing House of the Romanian Academy (Editura Academiei Române), Bucharest, 2013, pp. 179-196.

4. S.V. Stolyar, O.A. Bayukov, Yu.L. Gurevich, E.A. Denisova, R.S. Iskhakov, V.P. Ladygina, A.P. Puzyr', P.P. Pustoshilov, M.A. Bitekhtina, Inorganic Materials 42, 763 (2006).
5. S.V. Stolyar, O.A. Bayukov, Yu.L. Gurevich, V.P. Ladygina, R.S. Iskhakov, P.P. Pustoshilov Inorganic Materials 43, 638 (2007).
6. Yu.L. Raikher, V.I. Stepanov, S.V. Stolyar, V.P. Ladygina, D.A. Balaev, L.A. Ishchenko, M. Balasoiu, Phys. of Solid State 52(2) 277 (2010).
7. M. Balasoiu, S.V. Stolyar, R.S. Iskhakov, Yu.L. Raikher, A.I. Kuklin, O.L. Orelovich, Yu.S. Kovalev, T.S. Kurkin, G.M. Arzumanian, Romanian Journal of Physics 55(7-8), 782-789 (2010).
8. L.A. Ishchenko, S.V. Stolyar, V.P. Ladygina, Yu.L. Raikher, M. Balasoiu, O.A. Bayukov, R.S. Iskhakov, E.V. Inzhevatkin, Physics Procedia 9, 279-282 (2010).
9. M. Balasoiu, L.A. Ishchenko, S.V. Stolyar, R.S. Iskhakov, Yu.L. Raikher, A.I. Kuklin, D.V. Soloviov, T.S. Kurkin, D. Aranghel, G.M. Arzumanian, Optoelectronics and Advanced Materials – Rapid Communications, 4(12), 2136-2139 (2010).
10. L. Anghel, M. Balasoiu, L.A. Ishchenko, S.V. Stolyar, T.S. Kurkin, A.V. Rogachev, A.I. Kuklin, Y.S. Kovalev, Y.L. Raikher, R.S. Iskhakov, G. Duca, Journal of Physics: Conference Series, 351, 012005, (2012).
11. C.G. Chilom, D.M. Găzdaru, M. Bălăsoiu, M. Bacalum, S.V. Stolyar, A.I. Popescu, Romanian Journal of Physics 62, 701(13) (2017).
12. V.L. Aksenov, V.P. Glazkov, S.E. Kichanov, D.K. Pogoreliy, K.M. Podurets, V.A. Somenkov, B.N. Savenko, E.V. Yakovenko, Nucl Instr Meth A 575, 266-268 (2007).
13. S. Gomez, A. Garcia, T. Landete-Castillejos, L. Gallego, D. Pantelica, A. Pantelica, E.A. Preoteasa, A. Scafes, M. Straticiuc, Nucl Instr Meth B 371, 413-418 (2016).
14. J.A. Maxwell, J.L. Campbell, W.J. Teesdale, Nucl Instr Meth B 43 218-230 (1989). doi:10.1016/0168-583X(89)90042-6
15. J.R. Tesmer, M. Nastasi, Handbook of Modern Ion Beam Materials Analysis. Materials Research Society, Pittsburg, Pennsylvania, USA (1995).
16. J.F. Ziegler, J.P. Biersack, SRIM-2013, The Stopping and Range of Ions in Matter, http://srim.org/SRIM/SRIMLEGL.htm
17. L.R. Doolittle, Nucl Instr Meth B 15 (1-6) 227-231 (1986) doi: 10.1016/0168-583X(86)90291-0